Moving gold atoms with an atomic-force-microscope tip: A study of dimer and trimer formation on NaCl(100)

X. Bouju
Laboratoire de Physique Moléculaire, Université de Franche-Comté, 25030 Besançon Cedex, France

C. Joachim
CEMES-LOE, 29 Rue Jeanne Marvig, Boîte Postale, 4347, 31055 Toulouse Cedex, France

C. Girard
Laboratoire de Physique Moléculaire, Université de Franche-Comté, 25030 Besançon Cedex, France
(Received 22 November 1993; revised manuscript received 10 May 1994)

Recently it was demonstrated that the manipulation of atoms with the tip apex of a scanning probe microscope is a promising tool for the fabrication of nanometer-scale structures. We report time-dependent calculations of the motion of gold atoms on the NaCl(100) surface occurring after the collision with the tip of an atomic-force microscope (AFM). The interaction between the adsorbates and the tip-sample junction is calculated by considering a summation of pairwise potentials. The time-dependent trajectories of the adsorbed species are then derived from a classical dynamical dissipative method. Within this framework, the possibility of moving a single gold atom is investigated. We have also studied the formation of gold dimers and trimers from such manipulations. The stability of such clusters is discussed, in particular, its dependence on the initial position of the AFM tip. The range of tip-surface distances, which allows a controlled manipulation, has been determined.

I. INTRODUCTION

When the tip of a scanning tunneling microscope (STM) is scanned over a surface decorated with adsorbates, the mechanical interaction introduced by the tip apex can be larger than the electronic interaction stabilizing the adsorbed species on specific surface sites. As was first demonstrated by Eigler and Schweizer, the force exerted by this apex on an adsorbate can be very well controlled by using STM devices.[1] More recently, a similar procedure was used to slide Pt atoms and CO molecules on the Pt(111) surface.[2] This sliding process has been attributed to an attractive van der Waals trap induced by the tip apex when it is located just "on top" of the adsorbate.[3,4]

The atomic-force microscope (AFM) also appears to be an interesting alternative for manipulating metallic atoms, organic molecules, and aggregates deposited on the surface of insulating materials.[4] For example, it is well known that large adsorbates like proteins can be dragged away with the tip of an AFM.[5] Currently, the control of the interaction generating such a motion is not precise enough to allow manipulation of a single atom in the manner which has been achieved with a STM device. This would require the construction of an AFM machine with a very accurate determination of the tip-surface distance Δz and a very fine control of the tip apex fabrication. Let us recall that, for an STM able to slide atoms, Δz is known with a precision close to 10^{-3} Å[1] and the tip apex can be fabricated with a single atom at its extremity.[6]

Nevertheless, the possibilities offered by improvements in AFM instrumentation can be explored theoretically, since tip-adsorbate interactions can now be well calculated taking into account the atomic structure and the chemical composition of both tip apex and surface.[7] Some of these possibilities have been listed in Ref. 4, e.g., the study of the forces between reactants originating from a surface reaction, the mapping of the potential between an atom and the surface, and the manipulation of metal atoms on an insulating substrate to fabricate wires of subnanometer section.

Recently, we have shown that the sliding of a gold (Au) atom on the NaCl(100) surface with a diamond tip apex cannot be an "on top" sliding process, as happens for Xe on Cu(110) or Ni(110) surfaces, but rather is a lateral sliding process which could be called a "pushing" process.[8] This singular behavior is due to the 0.190-eV Au surface diffusion barrier along the Na^+-Na^+ path, one order of magnitude larger than the 15-meV diffusion barrier for Xe along the (110) copper rows. In fact the van der Waals trap created by the diamond apex is not deep enough to compensate for the diffusion barrier height.[8] Consequently, one needs to bring the apex close to the surface without destabilizing the adsorbate in an uncontrolled manner. Adiabatic and time-independent calculations have shown that a lateral shift of the apex by half a surface unit cell along a Na^+-Na^+ path constitutes a possible approach. In that case, the effect of the apex interaction raises the Au atom slightly in its hollow site. This implies a decrease of the Au atom diffusion barrier height along the diffusion path, and the atom may then be pushed with the tip.[8] However, no time-dependent calculations of such a process have been made to confirm the validity of the described mechanism.

In this paper we report time-dependent calculations of

gold atom motions on the NaCl(100) surface after collision with an AFM tip. The same diamond-tip-Au-NaCl(100) junction used in our preliminary static study[8] will be adopted in the present calculation, since the various interaction potentials have already been checked. This time-dependent approach is applied to the collision between an isolated Au atom pushed by the tip and another single Au atom or an Au dimer at rest on the surface. In fact because of the metallic cohesion between adsorbed species, one deals with a reactive collision process which results in the production of a dimer or trimer of gold atoms. We note that such a sequence of physical mechanisms would be interesting to study experimentally, since the reactants and the final product are well identifiable using the current AFM image capabilities in UHV.

The paper is organized as follows. The Au-NaCl(100), the Au-diamond apex, and the Au-Au interaction potentials are presented in Sec. II. A dissipative classical dynamical method is used in Sec. III to calculate the time-dependent trajectories of the Au atoms. The influence of the tip apex size on the pushing process of Au atoms on NaCl(100) will also be considered. Lateral and frontal dimer and trimer formations will be reported in Sec. IV. Finally, AFM constant height images of the reactants and of the products will be presented to facilitate their experimental recognition. Further extensions of this work will be proposed in Sec. V.

II. DIAMOND APEX-AU-NaCl(100) INTERACTION POTENTIALS

Before undertaking a studying of the time-dependent trajectories of an isolated Au atom pushed by the tip, an energy-based description of the tip apex-Au-NaCl(100) mechanical junction has to be considered. In such a junction, the tip apex is described as a finite diamond cluster structured in a C_{3v} symmetry, and the NaCl material by a finite slab composed of five layers (Fig. 1). The structure of both the tip apex and the NaCl(100) slab have been previously optimized separately using standard routines of molecular mechanics.[7,9] For the apex structure, most of our calculations have been performed with a cluster of 13 carbon atoms structured in four layers, and some with a 128 carbon atom cluster to check the validity of the 13-atom cluster results. There are 289 atoms per layer in the chosen NaCl(100) slab. In the junction, the Au atoms will be free to find their final equilibrium positions on NaCl(100); these positions depend on the tip-sample distance (Z_p) to the lateral position (X_p, Y_p). The distance Z_p can vary to keep the interaction force between the apex and the surface constant during the scanning of the surface in a constant force regime. These changes in equilibrium position are controlled by interactions between all the atoms in the junction. The apex and the NaCl(100) slab are assumed to be rigid after their independent full structure optimization. The total energy $U_{\text{total}}(\mathbf{R}_{ai},\mathbf{R}_j,\mathbf{R}_\alpha)$ of the junction can then be reduced, in a first approximation, to the sum of pairwise interaction potentials between atoms:

$$U_{\text{total}}(\mathbf{R}_{ai},\mathbf{R}_j,\mathbf{R}_\alpha)=U_{ps}(\mathbf{R}_j,\mathbf{R}_\alpha)+U_{pa}(\mathbf{R}_{ai},\mathbf{R}_j)+U_{as}(\mathbf{R}_{ai},\mathbf{R}_\alpha)+U_{aa}(\mathbf{R}_{ai}) \quad (1)$$

The tip apex to the NaCl(100) slab $U_{ps}(\mathbf{R}_j,\mathbf{R}_\alpha)$ potential is given by the usual summation of Buckingham terms:

$$U_{ps}(\mathbf{R}_j,\mathbf{R}_\alpha)=\sum_{j,\alpha}[A_{j\alpha}\exp(-|\mathbf{R}_j-\mathbf{R}_\alpha|/\lambda_{j\alpha})-C_{j\alpha}/|\mathbf{R}_j-\mathbf{R}_\alpha|^6] . \quad (2)$$

The vectors $\mathbf{R}_j$ represent the coordinates of the carbon atoms, and the $\mathbf{R}_\alpha$ those of the Na^+ or Cl^- ions of the NaCl(100) slab. The $A_{j\alpha}$, $\lambda_{j\alpha}$, and $C_{j\alpha}$ are calculated following the usual approximation:[10] $A_{j\alpha}=2.9\times10^5(A_jA_\alpha)^{1/2}$, $\lambda_{j\alpha}=(\lambda_j+\lambda_\alpha)/12.5$, and $C_{j\alpha}=2.25(\lambda_j+\lambda_\alpha)^6(A_jA_\alpha)^{1/2}$. The optimized constants are $A_\alpha=0.079$ kcal/mol and $\lambda_\alpha=0.9393$ Å for Na^+, $A_\alpha=0.238$ kcal/mol and $\lambda_\alpha=2.27$ Å for Cl^-, and $A_j=0.044$ kcal/mol and $\lambda_j=1.90$ Å for apex carbon atoms. This leads to $A_{j\alpha}=17097.7$ kcal/mol, $\lambda_{j\alpha}=0.2271$ Å, and $C_{j\alpha}=69.498$ kcal Å^6/mol for the C-Na^+ interaction, and $A_{j\alpha}=29\,676.5$ kcal/mol, $\lambda_{j\alpha}=0.3336$ Å, and $C_{j\alpha}=1210.63$ kcal Å^6/mol for the C-Cl^- interaction.

The Buckingham potential is preferred to the Lennard-Jones one since it leads to a better agreement between experimental and calculated constant force AFM images of the NaCl(100) surface at low applied forces.[9] Notice that our optimized NaCl(100) slab presents a rumpled surface, with the Na^+ ions calculated to be depressed by 0.089 Å in the surface relative to the Cl^- ions surface layer. The experimental value given for this rumpling distance is 0.0874 Å.[11]

The tip apex-Au atom potential $U_{pa}(\mathbf{R}_{ai},R_j)$ is also chosen as a sum of Buckingham terms:

$$U_{pa}(\mathbf{R}_{ai},\mathbf{R}_j)=\sum_{i,j}[A_{ij}\exp(-|\mathbf{R}_{ai}-\mathbf{R}_j|/\lambda_{ij})-C_{ij}/|\mathbf{R}_{ai}-\mathbf{R}_j|^6] . \quad (3)$$

A_{ij}, λ_{ij}, and C_{ij} are calculated using generalized parameters for metals from the MM2 molecular mechanics rou-

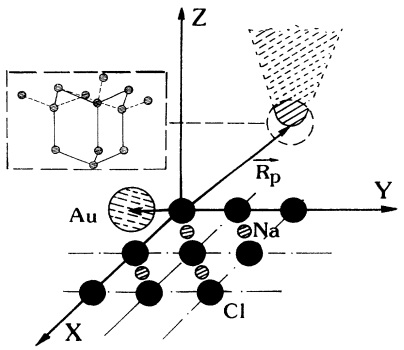

FIG. 1. Detail structure of the tip apex-gold atom-NaCl(100) surface junction used in the present paper. The diamond tip is limited to a C_{3v} apex of 13 atoms with a (111) orientation. The NaCl material is a finite slab of five layers with 289 atoms by layer with a standard 3.98-Å lattice parameter.

tine:[12] $A_{ij}=37\,600.8$ kcal/mol, $\lambda_{ij}=0.3576$ Å, and $C_{ij}=2328.7$ kcal Å^6/mol. Apart from a possible weak van der Waals bonding between the tip apex and an Au atom, no chemical bond between the two interacting systems is allowed for in (3). This choice is justified by the fact that the surface holding energy U_{as} of the adsorbate is large enough to prevent, at the tip apex to the Au distance considered here, the formation of an Au-C chemical bond.

The Au-NaCl(100) interaction is described by a potential of Lennard-Jones type:

$$U_{as}(\mathbf{R}_{ai},\mathbf{R}_{\alpha})=\sum_{i,\alpha}\left[-\frac{C_6}{|\mathbf{R}_{ai}-\mathbf{R}_{\alpha}|^6}-\frac{C_8}{|\mathbf{R}_{ai}-\mathbf{R}_{\alpha}|^8}-\frac{C_{10}}{|\mathbf{R}_{ai}-\mathbf{R}_{\alpha}|^{10}}+\frac{C_{12}}{|\mathbf{R}_{ai}-\mathbf{R}_{\alpha}|^{12}}\right]. \quad (4)$$

It was shown by Fuwa *et al.*[13] that Au atoms are weakly chemisorbed on the NaCl(100) surface with a bonding energy reaching about 0.7 eV. The semiempirical potential (4) proposed first by Chan, Buckingham, and Robins[14] reproduces accurately the Au bonding properties on NaCl(100). The repulsion constant C_{12} and the various dispersive strength coefficients occurring in this potential are available in Refs. 15 and 16. When the rumpling effect is included in our calculations, the diffusion barrier along the Na^+ rows reaches about 0.19 eV, and the equilibrium site of the gold atom is calculated to be directly above a Na^+ site.[8]

In order to describe the Au-Au interaction, we have chosen a Gupta-type potential in which a standard Born-Mayer term is compensated for with a pseudo-many-body contribution introduced to mimic the metallic cohesion:[17,18]

$$U_{aa}(\mathbf{R}_{ai})=E\sum_j\left\{A\sum_i\exp[-p(|\mathbf{R}_{ai}-\mathbf{R}_{aj}|-r_0)]-\left[\sum_i\exp[-2q(|\mathbf{R}_{ai}-\mathbf{R}_{aj}|-r_0)]\right]^{1/2}\right\}. \quad (5)$$

This potential reproduces in a satisfactory way the geometry of small Au clusters with the following parameters: $r_0=2.884$ Å (the bulk interatomic distance), $pr_0=10.3$, and $qr_0=4.0$. E and A were determined to fit the bulk cohesive energy per atom. This leads to $E=3.57$ eV and $A=0.1135$.[19]

We have tested this potential for small Au_n clusters ($n=2$–7). Apart from the Jahn-Teller distortion, the ground-state geometries of these clusters were found to be nearly identical to those obtained from *ab initio* calculations.[20,21] This distortion implies a less symmetrical geometry than the Gupta potential could predict. For Au_3, an equilateral triangle configuration is found by using the potential in Eq. (5), whereas *ab initio* calculations lead to an isosceles triangle configuration for the ground state.[20] This feature is well known from calculations on alkali clusters.[22] Concerning the tetramer, recent theoretical works on the Cu, Ag, or Au clusters have shown that the rhombus pattern is the most stable geometry,[23] in analogy with the case of other metals having a single valence electron.[24] The calculated bond length in the tetramer is 2.73 Å, whereas the Gupta potential leads to 2.5 Å. For larger aggregates, the pentamer displays a plane trapezium equilibrium structure with the potential in Eq. (5) rather than a trigonal bipyramid or a square pyramid. The calculated Au_6 conformation is a pentagonal pyramid,[25] and that of Au_7 is a pentagonal bipyramid. In spite of the rather good agreement the bond lengths calculated with Eq. (5) are generally too short compared to the experimental results or to more sophisticated calculations.[20] This means that the metallic cohesion allowed for in Eq. (5) is too large. It is possible to adjust the parametrization in Eq. (5) for each n value, but this would be artificial. Consequently, we have preferred to retain the standard parameters, since for our manipulation study only a reasonable prediction of the cluster conformation is required.

III. MOVING AN ISOLATED GOLD ATOM WITH A DIAMOND TIP

A. The equation of motion

The process proposed to move a single gold atom is based on a lateral interaction between a diamond apex and the adsorbate. From a time-dependent point of view, such a process can be simulated by considering the atom as a classical particle constrained to stay in the region of the tip-surface mechanical junction by a potential of the form (1). So the equation of motion of the gold atom near the tip is given by

$$m\frac{d^2\mathbf{R}_a(t)}{dt^2}+m\eta\frac{d\mathbf{R}_{\alpha}(t)}{dt}=-\frac{\partial}{\partial\mathbf{R}_a}U_{\text{total}}(\mathbf{R}_{\alpha}(t),\mathbf{R}_j(t),\mathbf{R}_{\alpha}), \quad (6)$$

where $\eta=\tau^{-1}$ is a friction constant and m the Au atom mass. U_{total} is now time dependent, since the position $\mathbf{R}_j$ of each apex atom changes with time to be able to push the Au atom. Moreover, the surface is assumed to be at 0 K. Consequently, there is no stochastic contribution to Eq. (6), in contrast to the usual model for the adsorbate surface diffusion.[26]

For an AFM (and for a STM), the experimental tip displacement speed is around 10 Å/s. So, on the time scale (10^{-13} s) of the low amplitude vibration of Au in a Na^+ hollow site, the tip does not move. This was the basis of our adiabatic and time-independent calculations concerning this process.[8] Therefore, the dynamical Eq. (6) has to be solved taking into account the difference of many orders of magnitude in the time scale. This is formally reminiscent of the calculation of protein conformations, where the time scale of the local vibrating bonds is very different form the one for a collective change of the whole protein conformation.[27] What helps in our case is the ac-

commodation time τ of Au on NaCl(100). The spatial extension of the migration of a "hot" Au atom on NaCl(100) is limited by friction effects. They come from the local polarization of the NaCl(100) surface around the instantaneous position of Au (time scale τ_e), and from surface phonon excitations (time scale τ_{ph}).

This accommodation time $\tau=\tau_e+\tau_{ph}$ is a time scale, allowing us to adjust the speed of the tip apex: as in usual experimental work, a motion of the apex must occur for a time Δt larger than τ. Unfortunately, neither experimental nor calculated τ values are available for Au on NaCl(100). For example, τ_e is obviously larger for chemisorbed species than for physisorbed ones: on an Ag surface, $\tau_e=3.3\times10^{-9}$ s for Xe atoms and $\tau_e=10^{-10}$ s for Ag adsorbates.[28] In the case of an insulating substrate, the estimation is less easy. We have chosen an intermediate value $\tau=2.0\times10^{-11}$ s for the Au-NaCl(100) system. In our calculation, the changing of tip position awaits the end of the Au atom relaxation. Thus a change in τ will not change our conclusion about the pushing process, but only some details in the time-dependent trajectories.

Equation (6) has been solved numerically for given initial positions of the tip apex at $\mathbf{R}_p=(X_p,Y_p,Z_p)$ and of gold atoms by applying a standard Verlet molecular dynamic algorithm.[29] Moreover, Δt has to be chosen to be around a tenth of the value of the period of the largest frequency of the vibration to be simulated in the system.

B. Movement of a single Au atom

From an experimental point of view and at low Au coverage, the Au clusters are accumulated along the cleavage steps of the NaCl(10) surface.[30] Some isolated Au atoms can be found on the atomically flat terraces between these steps.[31] Prior to any atomic manipulations, AFM images must be used to locate the Au atoms on the terraces. Very small scanning forces have to be used so as to leave each adsorbate in its equilibrium site. The threshold between the range of height to image and the range to manipulate is determined by the magnitude of the surface corrugations experienced by the adsorbate. In fact, what was a perturbation for the imaging process turns out to be an advantage for a controlled manipulation.[1]

For the sliding process currently used with a STM, the tip apex is positioned directly above the adsorbate atom.[1] This is the so-called "on top" configuration. If such a configuration is applied with an AFM in order to slide an Au atom on NaCl(100), the energy gain due to a weak apex touch on the adsorbate atom, i.e., one with $Z_p > 5.5$ Å, is much lower than the Au surface diffusion barrier height.[8] Reducing the apex-surface distance leads to a destabilization of the Au atom which is then constrained to move sideways to avoid the apex. This behavior is illustrated in Fig. 2. When the tip apex is displaced across the surface at fixed height $Z_p \leq 5.1$ Å, the atom jumps into another hollow site in a direction opposite to that of the apex displacement. As illustrated in Fig. 2, beyond this threshold value the Au atom avoids the apex but keeps its equilibrium site. These facts mean that the "on-top" tip adsorbate configuration does not allow controlled manipulations of a single gold atom adsorbed on NaCl(100).

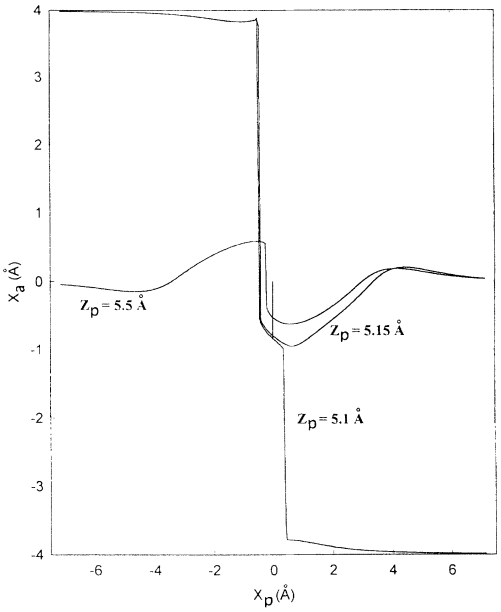

FIG. 2. The lateral position X_a of a gold atom along the Na^+ row is represented as a function of the lateral position X_p of the tip apex along the same row. At the beginning of the moving process, the apex is located just above the Au atom at a very large approach distance Z_p. This distance is then reduced toward its chosen value. This procedure explains the presence of the vertical line occurring just for $X_p=0$ Å. It corresponds to the time-dependent apex approach. After this preparation, the apex is scanned at a constant altitude along a Na^+ row of the crystal. For each tip-sample configuration the energy is minimized by considering three typical approach distances.

Let us now examine the pushing process in which the tip is positioned beside the gold atom in the same horizontal Na^+ row.[8] This configuration is illustrated in Fig. 3. The tip apex is first positioned 8 Å away from the Au atom on the Na^+ row axis corresponding to the Au equilibrium position. This is the initial condition for the

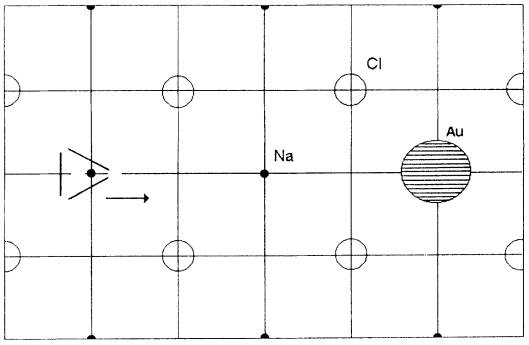

FIG. 3. Initial configuration used for the pushing process. The extremity (small grey circles) of the diamond tip apex is drawn on the NaCl(100) surface with the initial Au position (large circle with horizontal lines).

pushing process. Then, the height Z_p is slowly decreased until the chosen Z_p is reached. During that time, the Au atom adopts an equilibrium position in the apex-NaCl(100) junction. After this preparation, the tip is scanned along the Na^+ row direction at the chosen Z_p distance. Using this procedure, three kinds of Au atom motion have been obtained by solving the dynamical equation (6) (Fig. 4).

(i) For large Z_p ($Z_p \geq 5.36$ Å), the Au atom is not sufficiently trapped by the apex to be able to jump over the saddle point located between the two nearest Cl^- ions in order to reach the next hollow site. Therefore, due to its weak repulsion with the end tip atom when the apex passes over it, only a little backward destabilization can be expected. Finally, the atom returns to its initial hollow site when the tip passes on [Fig. 4(a)].

(ii) In a narrow range, 4.86 Å $\leq Z_p \leq 5.35$ Å, as the tip passes over the Au atom during the scan it ejects the atom backwards. In this case, the Au atom goes back to the nearest-neighboring equilibrium hollow site [Fig. 4(a)] due to a vertical pressure exerted by the tip apex. For example, with $Z_p = 4.86$ Å [Fig. 4(b)], the adsorption distance Z_a of the Au atom decreases continuously when the tip is scanned, until a certain threshold ($Z_a = 2.16$ Å) is reached. In this situation, the repulsion due to the atoms of the apex becomes too strong for the Au atom to stay in its initial equilibrium site. This results in the backward jump observed in Fig. 4(a).

(iii) Finally, for small Z_p ($Z_p \leq 4.85$ Å), the Au atom is sufficiently destabilized in its initial hollow site by the apex repulsion to produce a jump from its initial position to the next hollow site when the tip is scanned. The curves in Fig. 4(a) illustrate in a striking way the gradual and reproducible motion of the Au atom along the Na^+ row. A corresponding effect appears in Z_a, since to surmount the Cl^- saddle point, Z_a must increase. This explains the presence of the two narrow peaks at $X_p = -3.1$ and 1 Å observed in Fig. 4(b) when $Z_p = 4.0$ Å.

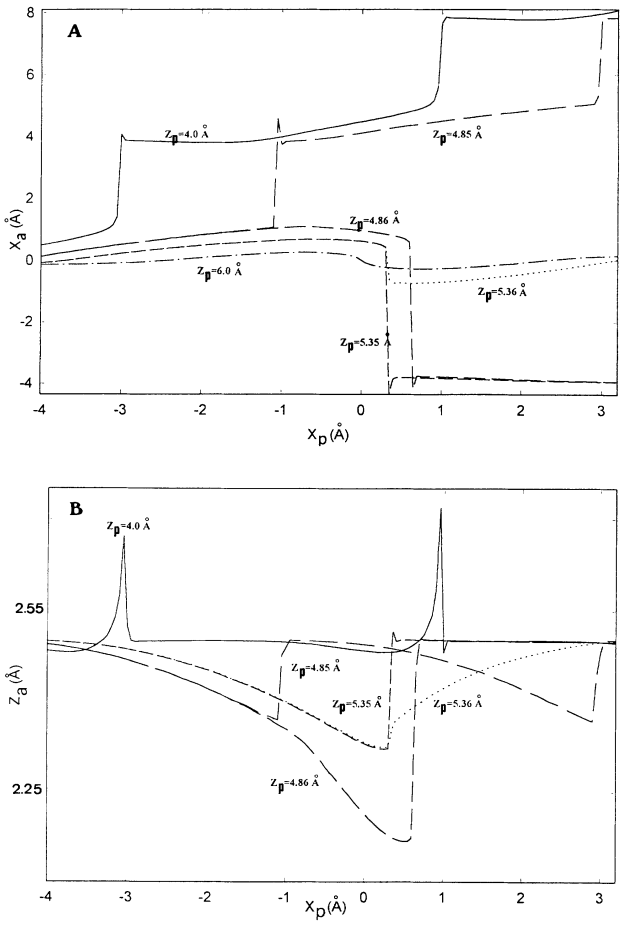

FIG. 4. Variation of both the lateral position X_a (curves *a*) and the corresponding altitude Z_a (curves *b*) of the Au atom as a function of the tip position X_p. As in Fig. 2, both the adsorbate and the tip move along a Na^+ row of the NaCl crystal. Different typical tip-surface heights Z_p have been considered. The initial configuration used to calculate this sequence is pictured in Fig. 3. At the beginning of the process the gold atom is located at the origin of the absolute frame just above a Na^+ site.

More details about the Au displacement induced by the tip are given by the time-dependent functions $X_a(t)$ and $Z_a(t)$. The time dependence of the Au trajectories do not appear in Fig. 4, since only the parametric curves $X_a(t) = f_x(X_p(t))$ and $Z_a(t) = f_y(X_p(t))$ are plotted. In Fig. 5, $X_a(t)$ and $Z_a(t)$ are presented, starting a few picoseconds before an Au jump via the neighborhood Cl^- saddle point, for a sliding tip with $Z_p = 3.0$ Å. The Au atom transfer occurs when X_a reaches about 4 Å, i.e., when Z_a decreases toward its 2.5-Å equilibrium position. This transfer is accompanied by damped oscillations in lateral and vertical positions due to the friction constant introduced in Eq. (6). The oscillation frequency of $X_a(t)$ is smaller than that of $Z_a(t)$ because of the large force constant which binds the Au atom on the surface, as compared to the force constant which keeps the gold atom in a hollow site.

As shown in Fig. 4, two distance thresholds ($Z_p = 4.85$ and 5.36 Å) are characteristic of the Au pushing process with a diamond tip on NaCl(100). This is summarized in Fig. 6 by representing the probability $P(Z_p)$ of such a push as a function of Z_p. For the "on top" sliding of a Xe atom on Ni(110), there is only one threshold altitude, $Z_p = 6.8$ Å,[32] defined as the altitude for which $P(Z_p) = 0.5$ for sliding. This was determined experimentally over a sequence of successful and unsuccessful sliding processes.[32] For the Au atom the existence of two different Z_p threshold backward and forward jumps, instead of the single threshold for the Xe atom, appears to be a consequence of the pushing process chosen. Since this process is determined by the height of the diffusion barrier, one may wonder if such a double threshold can be observed in STM by choosing an adsorbate-substrate combination displaying larger diffusion barrier height.

Another difference between our calculated $P(Z_p)$ curves and the experimental ones is the discontinuous $P(Z_p)$ variation in the threshold regions (Fig. 6). This is due to the fact that the Au surface tunneling is not considered in Eq. (6). In the threshold regions, the possibility for the Au atom to tunnel through the deformed diffusion barrier instead of jumping over it will smooth

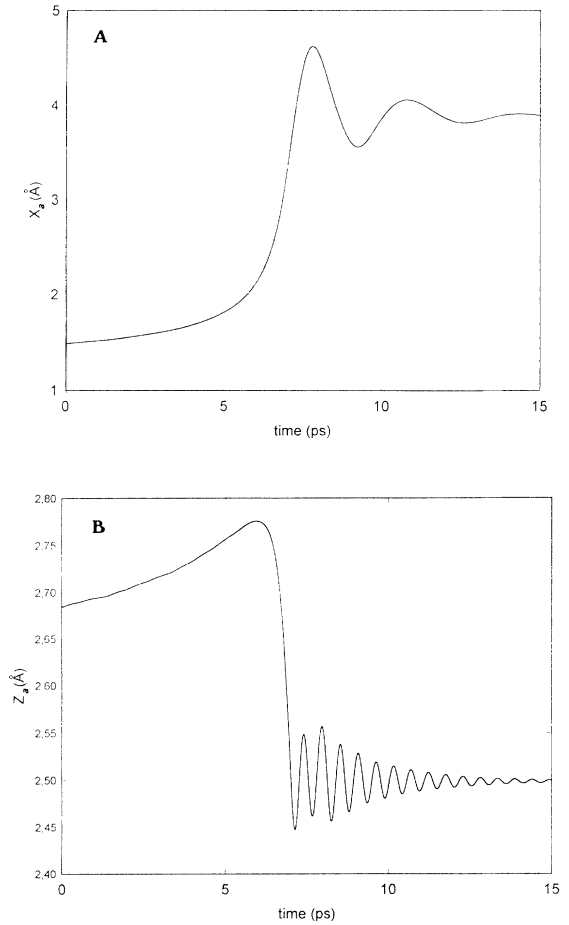

FIG. 5. Time variation of the coordinates $X_a(t)$ (curves *a*) and $Z_a(t)$ (curves *b*) of a single Au jumping from one equilibrium position to another one. The second equilibrium site is located along the same Na^+ row. We have considered a tip-sample distance $Z_p = 3$ Å and a tip motion speed of 21 Å/ns.

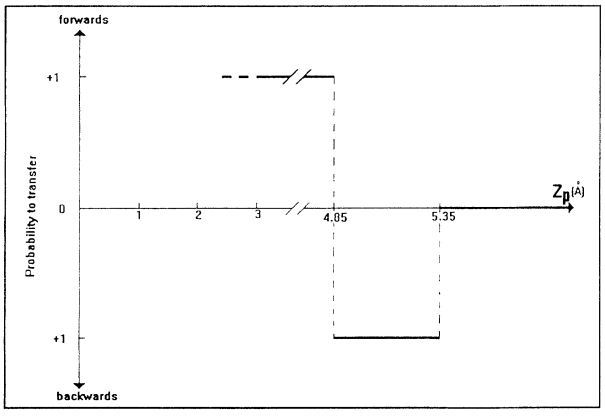

FIG. 6. Probability $P(Z_p)$ of obtaining a successful push of the Au atom as a function of the tip-sample distance Z_p. In the forward case, the function $P(Z_p)$ clearly indicates a whole displacement along the initial Na^+ row. In the backward case, the atom jumps in the opposite direction from the tip motion. Note that in the framework of a whole quantum-mechanical calculation, the vertical transitions ocurring in the variation of $P(Z_p)$ should be smoothed by the surface tunneling effects.

the variation of $P(Z_p)$. This effect is found experimentally for the Xe $P(Z_p)$ curves.[32]

Equation (6) was also solved with a larger tip apex of 128 carbon atoms, while keeping the same C_{3v} 13-atom apex at the end. No significant change was found in the result. The attractive contribution introduced by the additional tip atoms does not change the main features of the manipulation process described above. The only difference lies in a weak shift of the two distance thresholds: 4.81 Å instead of 4.86 Å, and 5.31 Å instead of 5.36 Å.

IV. Au DIMER AND TRIMER FORMATION

When a beam of particles composed of atoms or small clusters is focused on a surface, the first clustering of adsorbates occurring at a given temperature depends dramatically on a subtle competition between the atom-atom interactions, the adsorbate holding energy, and the initial kinetic energy of each adsorbate.

As recently observed by Weiss and Eigler for the Xe-Pt(111) system, "hot" Xe atoms may diffuse over hundred of Å before being accommodated.[33] The Xe atoms accumulate preferentially near the step edges and the structural defects of the Pt(111) surface. To overcome this spontaneous organization, one must wait for the accommodation and, at very low temperature, use a STM tip to slide the Xe atoms, one by one, in order to fabricate artificial structures.[1] In the case of Xe adsorbates, the weak lateral interactions between them prevent any clustering processes. For Pt atoms on Pt(111), artificial constructions such as atomic lines can also be assembled, using the sliding process.[2] At low temperature (4 K), the displacement barrier height [about 0.2 eV for Pt on Pt(111)] seems to be sufficiently large to avoid a spontaneous reorganization[34] even after the construction of a close-packed linear chain.[2] At higher temperature, this reorganization will occur via the random motion of surface atoms or via hopping and will lead to cluster formation.

For the Au-NaCl(100) system, it is well known that clustering also occurs at the step edges.[30,31] Unlike what happens for the Pt-Pt(111) system, even at very low temperature, the competition between the 0.19-eV Au diffusion barrier height and the Au-Au interaction given by Eq. (5) will not permit the use of such artificial fabrication processes to form close-packed atomic metallic lines on NaCl(100).

In Sec. IV A and IV B, the dynamical equation (6) will be solved for two and three gold atoms located in the tip-substrate junction. At the beginning of the simulation a single gold atom will be pushed by a diamond tip apex formed of 13 carbon atoms, and the others will be considered at rest. Let us note that in this simulation the damping of the Au-Au bond vibration has been taken to be identical with that of a single Au atom adsorbed on NaCl(100).

A. Au_2 formation

From the Gupta potential [Eq. (5)], an isolated Au_2 dimer has a bond length of 2.31 Å, a little too short com-

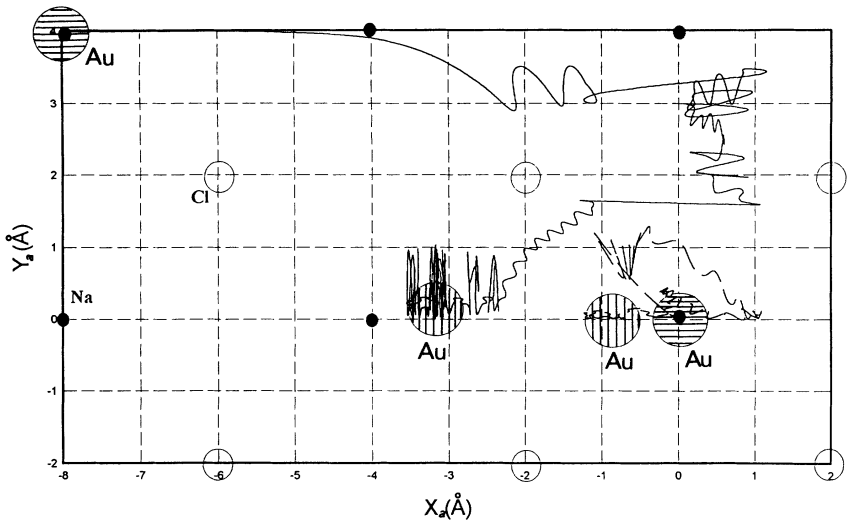

FIG. 7. Initial (circles with horizontal lines) and final (circles with vertical lines) positions of the Au atoms on NaCl(100) before and after a collision of two gold atoms. The full and dashed lines are an example of a possible time-dependent trajectory. In this simulation the tip speed is 80 Å/ns, and the duration of the represented trajectories is 0.06 ns.

pared to recent *ab initio* calculations[20] and evaluated data obtained from experiments.[35] On NaCl(100) at very low temperature, two isolated Au atoms will stay in their respective hollow sites if their relative distance is greater than 8 Å.[36] Using Eq. (5), the equilibrium position of Au_2 on NaCl(100) has been calculated. The Au-Au 2.32-Å distance on NaCl(100) is a little larger than that in the gas phase, due to the mismatch between the NaCl(100) lattice constant and the 2.31-Å bond length of Au_2 in the gas phase. Furthermore, there is no symmetry breaking at our level of approximation. The two atoms formed a dimer centered on the saddle point in a direction perpendicular to the Cl^--Cl^- direction.

Starting with the Au atoms far apart, there are two different ways of sliding one of them in the direction of the other: a lateral approach or a frontal approach.

For the lateral approach, the two Au atoms are adsorbed on two different parallel Na^+ rows. The tip is then positioned laterally with respect to the Au atom to be moved, and Eq. (6) is solved for a tip motion in the row parallel to the row occupied by the stationary Au atom. Only configurations with two consecutive rows have been investigated (Figs. 7 and 8). A typical trajectory of the two Au atoms during both the approach and scattering processes is drawn in Fig. 7. In this case, the speed of the tip is 80 Å/ns and $Z_p = 4.85$ Å. A detailed analysis of this trajectory shows that initially the pushed atom is attracted by the stationary atom (located at the origin in Fig. 7). We note that during this first part of the collision, the stationary Au atom is slightly attracted by the pushed one, and is then repelled when the first Au atom crosses the saddle point. Constrained by the second gold atom, the apex, and the Cl^- row, the pushed atom escapes backwards into another equilibrium site. The result of this reactive collision is the formation of a dimer parallel to the Na^+ horizontal rows. In Fig. 7, the duration of the atom trajectory is 0.06 ns, which represents a speed of the gold atom four times larger than the tip speed. During the collision, the tip is situated at $X_p = -8.6$ Å, so as not to disturb the scattering process. After that, the tip apex follows its straight trajectory without perturbing the dimer structure.

When the speed of the tip is reduced with the same approach distance $Z_p = 4.85$ Å, the final orientation of the Au_2 dimer changes. In fact, in this situation the pushed Au atom does not obtain enough energy from the tip to overcome the Cl^- barrier. As presented in Fig. 8 for a speed of 20 Å/ns, a dimer is first formed (circles with ob-

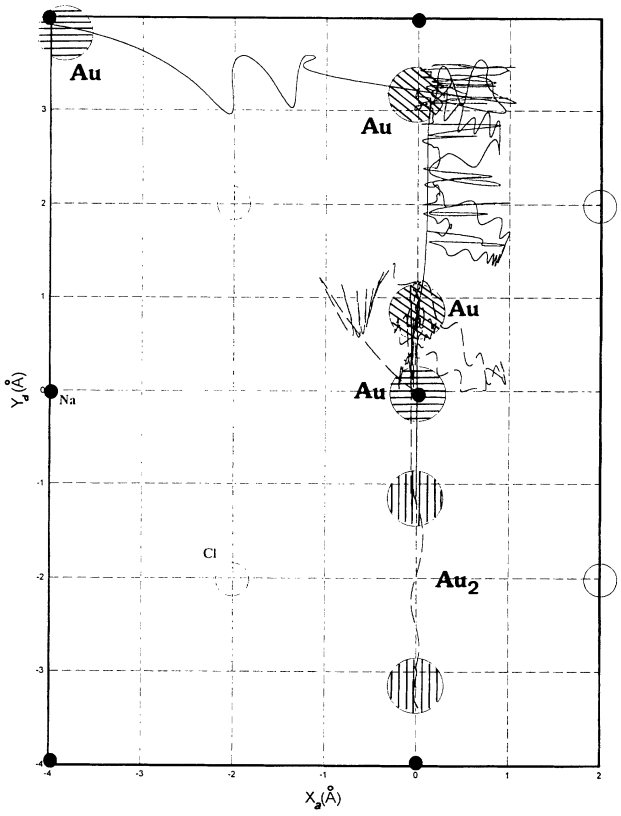

FIG. 8. Another example of time-dependent trajectories for the two gold atoms during an Au-Au collision induced by an apex push of one Au on NaCl(100). In this second application the tip speed is 20 Å/ns, and the duration of the represented trajectories is 0.5 ns. The circles with horizontal, oblique, and vertical lines schematize, respectively, the initial, intermediary, and final positions of the two Au atoms.

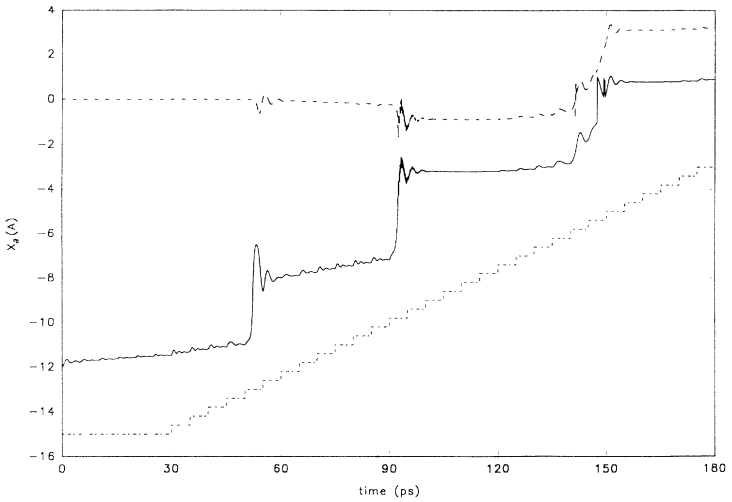

FIG. 9. Time-dependent representation of an Au-Au frontal collision. The motion of the apex and the two gold atoms is represented by the variation of the coordinate $X_a(t)$ along a sodium row of the surface. The dashed line describes the motion of the stationary atom after the collision; the full line characterizes the movement of the atom pushed by the tip. The initial positions are -12 Å for the pushed atom and 0 Å for the stationary Au. The tip speed is fixed at 80 Å/ns, and its successive positions are represented by the stepped dashed line.

lique lines in Fig. 8). Subsequently, this dimer rapidly perturbed by the tip apex, since the pushed gold atom has been stabilized after starting from the next Na^+ row. The stationary Au atom passes over the Cl^- row via a saddle point to reach the next hollow site in the consecutive Na^+ row. Then the pushed Au atom occupies the initial hollow site left by the other Au atom. The result of this collision is the formation of a dimer along the Na^+ vertical row (circles with vertical lines in Fig. 8), with the same structure and energy as that formed at a higher speed of the tip.

In a frontal approach (cf. Fig. 9), the two Au atoms and the tip are aligned on the same Na^+ horizontal row. The initial condition is chosen with the stationary Au atom at $X=0$ Å and the pushed one at $X=-12$ Å. The tip is prepared at $Z_p=4.85$ Å as described previously, and the sliding process is started 30 ps afterward (Fig. 9). Here we have chosen a time-dependent representation instead of one based on trajectory, since all the motions are constrained on the same axis. This is due to the fact that the push on the Au atom is weak enough to prevent any lateral escape. At the first Au atom jump from -12 to -8 Å (Fig. 9), the position of the stationary Au is slightly perturbed. At the second jump, the Au_2 dimer is formed and the Au-Au distance is quickly stabilized at 2.32 Å. One remarks that the tip continues to move after the Au_2 dimer formation. Therefore, the whole dimer is pushed at the next jump, as presented in Fig. 9, and will continue to be pushed until the retraction of the tip.

B. Au_3 formation

From the Gupta potential described in Eq. (5) the ground-state geometry of an isolated trimer Au_3 is an equilateral triangle with a 2.48-Å bond length. The equilibrium position of the Au trimer on NaCl(100) is presented in Fig. 10 (circles with vertical lines). The bond length is not changed from the gas phase due to the fact that already for the trimer the cohesive energy dominates the substrate contribution.

The initial conditions for the collision are presented in Fig. 10. The Au atom to be pushed and the stationary Au_2 dimer are chosen in the same Na^+ row (circles with horizontal lines). The initial distance between the two adsorbates is about 8 Å to avoid any mutual attraction. The bond length in Au_2 is 2.32 Å and $Z_p=4.85$ Å.

The trajectories of the Au atoms are presented in Fig. 10. Upon collision with the pushed Au[Au(3)], the front atom of the dimer [Au(2)] is laterally repelled and reaches the Cl^- row. It passes over the Cl^--Cl^- saddle point and can escape from its original Na^+ row into the next one. But due to its attraction to the two other Au atoms, Au(2) is stabilized on the saddle point with an altitude above the surface larger (2.78 Å) than those for Au(1) (2.65 Å) and Au(3) (2.68 Å). This position is controlled by the motion of the Au(1) atom, which upon collision is attracted by Au(2) and Au(3) along the Na^+ row. At the same time, Au(3) follows the direction of the Na^+ row and finds its equilibrium position between the saddle point and the Na^+ hollow site. The result of this collision is the formation of a trimer (circles with vertical lines in Fig. 10) with an equilateral conformation, as in the gas phase. In the calculation, the motion of the tip was stopped after the full relaxation of this trimer geometry.

If the apex continues its motion, successive positions of Au_3 are represented in Fig. 11. The Au(3) atom is repelled sideways by the tip since it is higher in altitude than on a hollow site. This results in a complete reorgan-

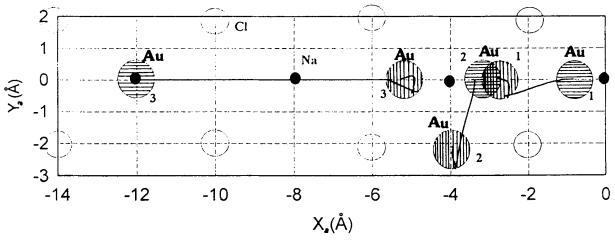

FIG. 10. An example of time-dependent trajectories of three Au atoms during an Au-Au_2 collision induced by the AFM tip. The circles with horizontal lines are the initial Au atom positions, and those with vertical lines represent the final atomic positions. The tip speed is fixed at 80 Å/ns, and the duration of the represented trajectories is 0.06 ns.

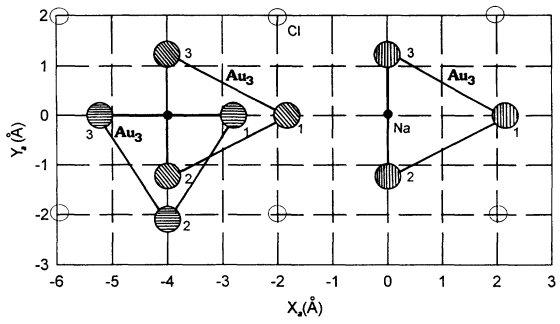

FIG. 11. A sequence of different equilibrium positions of a gold trimer on NaCl(100) induced by the tip displacement along a Na^+ row of the surface. The circles with horizontal lines schematize the gold atoms after the collision when the tip is located at the position $X_p = -14.8$ Å. When the tip continues its straight motion, a reorganization of the trimer occurs (circles with oblique lines, $X_p = -8.8$ Å). Finally, the tip apex pushes the Au_3 cluster (circles with vertical lines, $X_p = -4.8$ Å). The tip height used in this simulation is $Z_p = 4.85$ Å.

ization of Au_3, since a lateral push on Au(3) leads to a displacement of Au(2) and Au(1) (circles with oblique lines in Fig. 11). Notice that, as for Au_2, Au_3 will be pushed as a whole trimer until the retraction of the tip.

The trajectories during the Au_3 formation are less chaotic than those during Au_2 formation. This is due to the fact that Au_2 creates a deeper and larger potential well than a single atom on NaCl(100). Therefore in this case, the trajectories are less sensitive to the details of the surface corrugations than those for a single stationary atom. One consequence is that there is no variation in the trajectories as a function of the initial speed of the tip for a given Z_p. When Au(3) enters the region of the attractive potential created by Au_2, the gradient of the potential energy is large enough to control the Au(3) gain in kinetic energy independently of the initial tip speed.

To help in the recognition of Au_2 and Au_3 on NaCl(100), constant distance AFM images of these adsorbates have been calculated. A height of $Z_p = 5.5$ Å was chosen in order to leave the clusters in their equilibrium

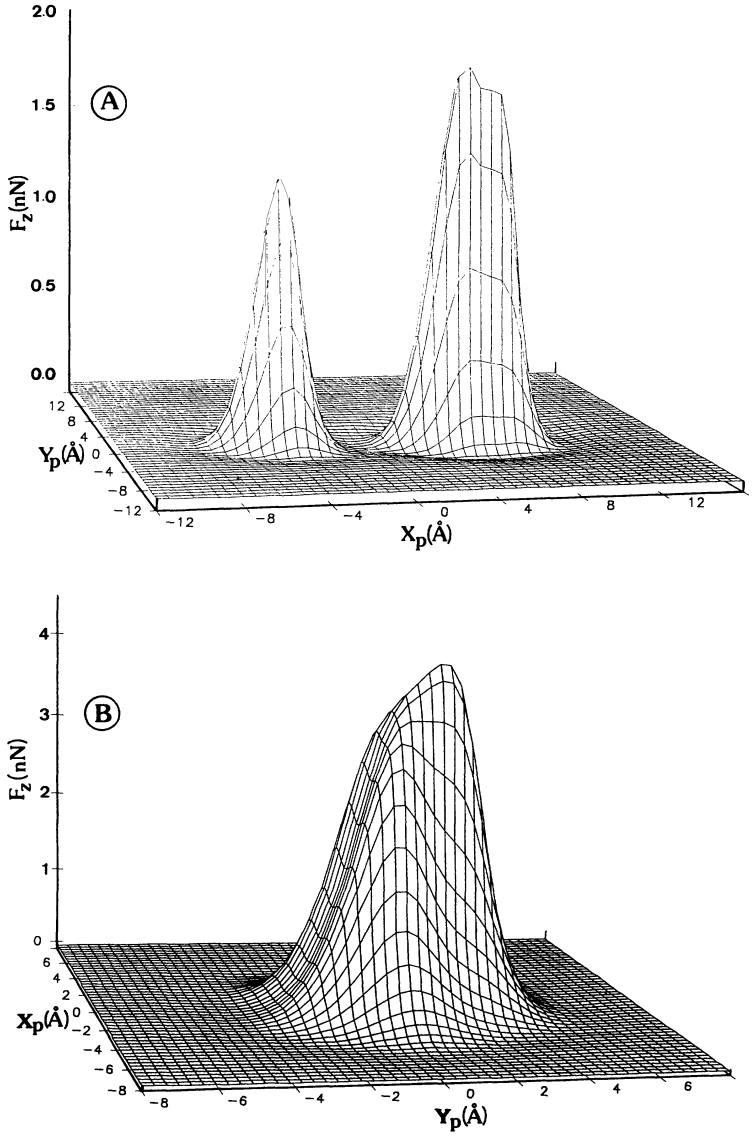

FIG. 12. Constant distance AFM images of Au, Au_2, and Au_3 on NaCl(100). The structure of the tip for this simulation is represented on Fig. 1. In order to minimize the apex-cluster interaction, these images have been calculated at a distance $Z_p = 5.6$ Å. The first AFM map (a) gives some indication on the surface topography before the collision. The second map (b) represents the AFM image of the trimer after the collision.

position upon scanning. At this distance, the atomic structure of the NaCl(100) surface is not resolved (Fig. 12). Notice also that the AFM map of an isolated Au is not symmetric when imaged with a C_{3v} diamond apex [Fig. 12(a)]. This is due to the interaction of the second layer of the apex with Au atom.

The clusters show up as an asymmetrical bump on the surface. Nevertheless, it is difficult to identify precisely each Au atom composing the clusters; for example, to distinguish the two gold atoms in the Au_2 AFM map of Fig. 12(a). In this case, this is due to the short bond length and to the tip symmetry. Au_3 is more easily identifiable due to its triangular shape and to the presence of the atom Au(3) which has a higher altitude on the surface [Fig. 12(b)].

CONCLUSION

Depending on the surface diffusion barrier height, the tip apex of a STM may be used to slide or push an adsorbate. For a small barrier, the sliding process is very controllable, but for a large barrier a pushing process is preferable. To decide between the two processes, the heights of the barrier must be compared to the energy gain for an "on top" tip apex-adsorbate configuration.

For the Au-NaCl(100) system, we have shown, using time-dependent trajectory calculations, that the "pushing" of Au atoms with an AFM tip apex can be used to manipulate Au atoms on the surface and to fabricate Au dimers and trimers. Due to the metallic cohesion, the constructed trimer is not a close-packed linear chain but a triangular cluster as in the gas phase. Larger clusters may also be assembled, but their conformation is globular and does not extend in linear chains.

Further improvements of the presented calculations will involve a better description of the friction effect, the calculation of the surface tunneling effect when the diffusion barrier is deformed by the tip apex, and the deformation of the surface by the tip apex interaction.

ACKNOWLEDGMENTS

The authors express their sincere thanks to R. Poteau and F. Spiegelman for stimulating discussions on metal clusters during this work and to J. Killingbeck for a careful reading of the manuscript. The Laboratoire de Physique Moléculaire is "Unité Associée du Centre National de la Recherche Scientifique No. 772." The CEMESLOE is "Unité Propre No. 8011 au Centre National de la Recherche Scientifique."

[1]D. M. Eigler and E. K. Schweizer, Nature **344**, 524 (1990).
[2]P. Zeppenfeld, C. P. Lutz, and D. M. Eigler, Ultramicroscopy **42-44**, 128 (1992).
[3]X. Bouju, C. Joachim, C. Girard, and P. Sautet, Phys. Rev. B **47**, 7454 (1993).
[4]J. A. Stroscio and D. M. Eigler, Science **254**, 1319 (1991).
[5]A. S. Lea, A Pungor, V. Hlady, J. D. Andrade, J. N. Herron, and E. W. Voss, Jr., Langmuir **8**, 68 (1992).
[6]Vu Thien Binh and J. Marien, Surf. Sci. **202**, L539 (1988).
[7]H. Tang, C. Joachim, and J. Devillers, Surf. Sci. **291**, 439 (1993).
[8]C. Girard, X. Bouju, and C. Joachim, in *Computation for the Nanoscale,* edited by P. E. Blöchl, C. Joachim, and A. J. Fisher (Kluwer Academic, Dordrecht, 1993), p. 209.
[9]H. Tang, C. Joachim, J. Devillers, and C. Girard, Europhys. Lett. (to be published).
[10]R. B. Nachbar, Quantum Chemistry Program Exchange 514, Indiana University, Bloomington, IN.
[11]Y. Kashihara, S. Kimura, and J. Harada, Surf. Sci. **214**, 477 (1989).
[12]N. L. Allinger and Y. H. Yuh, Quantum Chemistry Program Exchange 395, Indiana University, Bloomington, IN.
[13]K. Fuwa, K. Fujima, H. Adachi, and J. Osaka, Surf. Sci. **148**, L659 (1984).
[14]E. M. Chan, M. J. Buckingham, and J. L. Robins, Surf. Sci. **67**, 285 (1977).
[15]C. Girard, Phys. Rev. B **43**, 8822 (1991).
[16]A. Lakhlifi and C. Girardet, J. Chem. Phys. **94**, 688 (1991).
[17]R. P. Gupta, Phys. Rev. B **23**, 6265 (1981).
[18]D. Tomanek, S. Mukherjee, and K. H. Bennemann, Phys. Rev. B **28**, 665 (1983).
[19]S. Sawada and S. Sugano, Z. Phys. D **20**, 259 (1991).
[20]C. W. Bauschlicher, S. R. Langhoff, Jr., and H. Partridge, J. Chem. Phys. **91**, 2412 (1989); **93**, 8133 (1990).
[21]V. Bonačić Koutecký, P. Fontacci, and J. Koutecký, Chem. Rev. **91**, 1035 (1991).
[22]J. Buttet, R. Car, and J. L. Martins, J. Chem. Phys. **78**, 5646 (1983); F. Cocchini, T. H. Upton, and W. Andreoni, *ibid.* **88**, 6068 (1988); U. Röthlisberger and W. Andreoni, *ibid.* **94**, 8129 (1991); U. Röthlisberger, W. Andreoni, and P. Gianozzi, *ibid.* **96**, 1248 (1992); R. Poteau and F. Spiegelmann, *ibid.* **98**, 6540 (1993).
[23]K. Balasubramanian and P. Y. Feng, J. Phys. Chem. **94**, 1536 (1990); H. Pleeby, I. Parras, L. G. Petterson, P. Siegbahn, and U. Wahlgren, *ibid.* **94**, 5471 (1990).
[24]J. Koutecký and P. Fantucci, Chem. Rev. **86**, 539 (1986).
[25]D. W. Liao and K. Balasubramanian, J. Chem. Phys. **97**, 2548 (1992).
[26]A. Zangwill, *Physics at Surfaces* (Cambridge University Press, Cambridge, 1988).
[27]J. A. McCammon and S. C. Harvey, *Dynamics of Proteins and Nucleic Acids* (Cambridge University Press, Cambridge, 1987).
[28]B. N. J. Persson, J. Chem. Phys. **98**, 1659 (1993).
[29]W. F. van Gunsteren and H. J. C. Berendsen, Angew. Chem. Int. Ed. Engl. **29**, 992 (1990).
[30]G. A. Basset, Philos. Mag. **3**, 1042 (1958); H. Bethge, *Interfacial Aspect of Phase Transition* (Reidel, Dordrecht, 1982), p. 669.
[31]H. Sato and S. J. Shinozuki, Appl. Phys. **41**, 3165 (1970); V. N. E. Robinson and J. L. Robins, Thin Solid Films **20**, 155 (1974).
[32]P. Zeppenfeld (private communication).
[33]P. S. Weiss and D. M. Eigler, Phys. Rev. Lett. **69**, 2240 (1992).
[34]D. W. Basset and P. R. Webber, Surf. Sci. **70**, 520 (1978).
[35]K. P. Huber and G. Herzberg, *Constants of Diatomic Molecules* (Van Nostrand Reinhold, New York, 1979).
[36]C. Joachim, X. Bouju, and C. Girard, in *Atomic and Nanometer Scale Modifications of Materials: Fundamentals and Applications,* edited by Ph. Avouris (Kluwer Academic, Dordrecht, 1993), p. 247.